JOURNAL OF CATALYSIS 125, 265–275 (1990)

Lanthanum Cobalt Oxide Oxidation Catalysts Derived from Mixed Hydroxide Precursors

K. R. BARNARD, K. FOGER, T. W. TURNEY,[1] AND R. D. WILLIAMS

CSIRO, Division of Materials Science and Technology, Locked Bag 33, P.O. Clayton, Victoria, Australia 3168

Received April 24, 1989; revised March 16, 1990

Simultaneous oxidation/co-precipitation of an equimolar mixture of La(III) and Co(II) nitrates afforded a hydroxide-containing gel, which was converted to $LaCoO_3$ on calcination at 600°C. A material with surface area in excess of 40 m^2/g has been produced, provided the hydroxide gel was washed with a nonaqueous solvent before dehydration. The resultant $LaCoO_3$ perovskite sintered readily on heating above 700°C. Rates for oxidation for CO and propane showed a linear dependence upon the surface area of $LaCoO_3$ in the temperature range RT to 600°C.

INTRODUCTION

Rare earth perovskite powders have potential commercial applications as electrode materials or in catalytic processes (*1, 2*). Sr-doped $LaCoO_3$ is particularly active, among the nonnoble metal catalysts, for the conversion of automotive exhaust emissions, i.e., oxidation of CO and hydrocarbons and reduction of CO with NO to produce CO_2 and N_2 (*2–5*).However, a major drawback to the use of perovskite-based catalysts, in general, is the inability to produce high-surface-area materials. Two strategies have been employed to improve the surface area:

(i) A conventional ceramic method involving firing and grinding a mixture of the component oxides generally affords areas of less than 2 m^2/g (*6*). With submicron grinding, the surface area of preformed $SmCoO_3$ powder has been increased from 3 to 30 m^2/g (*7*).

(ii) Preparative methods which rely on the thermal decomposition of compositionally homogeneous precursors have been extensively used. Precursor materials, such as mixed citrate, acetate, oxalate, or nitrate salts, transform to the corresponding perovskite phase at much lower temperatures than those required in the ceramic method (*6, 8–17*). Areas of between 4 and 50 m^2/g (after heating to at least 600°C) have been obtained by these methods for $LaCoO_3$. However, the samples with higher areas have often been prepared by nonroutine methods, such as supersonic atomization of solutions (*10*).

We have examined co-precipitation of a stoichiometric Co/La mixed hydroxide, in which simultaneous oxidation of Co(II) to Co(III) was induced by co-addition of an oxidizing agent, a method reported previously by Vidyasagar *et al.* (*18*). High-area samples can be obtained by this method only if the hydroxide gel is dehydrated in a controlled manner by washing with a water-miscible nonaqueous solvent. Subsequent calcination afforded a crystalline $LaCoO_3$ powder with a perovskite structure and a surface area largely determined by the calcination temperature. The dependence of CO and propane oxidation on the surface area of the powder has been examined and areal catalytic activities determined.

METHODS

Preparation of Precursor Gels

Hydrated cobalt(II) and lanthanum nitrates (20 mmol each) were dissolved in deoxygenated, deionized water (100 ml) and

[1] To whom all correspondence should be addressed.

0021-9517/90 $3.00

the solution added dropwise under a nitrogen atmosphere to a rapidly stirred solution of sodium hydroxide (7.2 g, 0.18 mol) in sodium hypochlorite (3.5 *M*, 30 ml). Use of an inert atmosphere minimized carbonate contamination in the final product. The resultant olive-green gel was washed repeatedly with warm, degassed, deionized water (9 × 80 ml) until the conductivity of the washings dropped to 1–3 mSm^{-1}. The material was then washed with AR acetone (3 × 50 ml) and dried under vacuum (2 days) to afford a brown powder. Typical elemental analysis—Found (wt%): Co, 22.7; La_2O_3, 65.7; Na, <0.1, giving a Co/La atom ratio of 0.96. Similar coprecipitations were performed with initial concentrations of 1, 0.02, and 0.002 *M* in Co and La, as well as where the NaOCl was omitted and by a completely sodium-free route, using Me_4NOH/H_2O_2 instead of NaOH/NaOCl (at $[Co^{2+}] = [La^{3+}] = 0.2$ *M*).

Perovskite Formation

Thermogravimetric analysis (TGA) of the precursor was performed using a Stanton–Reelcroft STA-780 analyser [N_2 atmosphere, ramp rate = 10°C/min]. Perovskite samples were prepared by heating the precursor at 400°C (1 h, in air) and then 600°C (1 h). The effect of temperature of the surface area of the perovskite was also examined by pretreating five samples prepared from the same batch (0.2 *M* metal concentrations) at 400°C (1 h), then calcining each individual sample at temperatures between 600 and 950°C for a further hour.

Characterization

Both the precursor and perovskite powders were examined by X-ray diffraction (XRD) [Siemens D500, using Co$K\alpha$ radiation, step scan size = 0.04°], by transmission electron microscopy (TEM) and electron diffraction [JEOL CX-100; samples ultrasonically dispersed in hexane and deposited on holey carbon grids] and by infrared spectroscopy [Mattson FTIR CYGNUS 100, using KBr disks; gel samples dried *in vacuo* (24 h, RT)]. Nitrogen adsorption isotherms [Carlo Erba 1800; measured at −196°C] were analyzed to give BET surface areas. Surface areas were also estimated from crystallite sizes, which were determined from the width of the $K_{\alpha 2}$-stripped, (024) X-ray diffraction lines, by using the Debye–Scherrer equation.

TABLE 1

Composition of Gas Reaction Mixture

Gas	Composition (vol%)
Propane	0.104 ± 0.002
CO	0.983 ± 0.020
O_2	1.44 ± 0.03
He	97.5

Catalyst Testing

Catalysts were tested in a quartz, fixed-bed reactor for the oxidation of a CO/propane mixture with composition as given in Table 1. The catalyst sample (75 mg, 60–100 mesh) was pretreated with oxygen (heat 10°C/min to 300°C; hold, 15 min), then helium, while the reactor cooled to ambient temperature. The gas mixture (flow rate = 24–26 ml/min) was then passed through the reactor, which was heated in a controlled manner at a rate of 4°C/min. On-line sampling for CO_2 and propane was undertaken at 20°C temperature intervals using gas chromatography [Varian 3700, 1 m Porapak T, CO_2 by TCD and propane by FID]. The CO remaining in the gas stream was calculated from the CO_2 and propane mass balances, using Eqs.(1) and (2). The mean values of two separate runs were used to calculate CO and propane oxidation to CO_2 as a function of temperature.

RESULTS

Precursor Preparation and Characterization

Simultaneous oxidation/co-precipitation of equimolar mixtures of Co(II) and La ni-

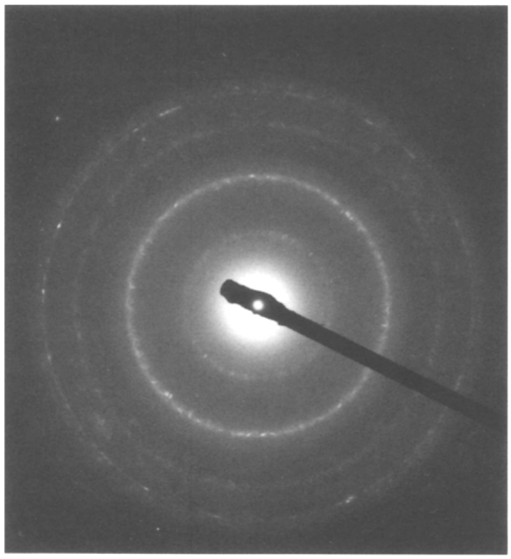

FIG. 1. Selected area electron diffraction pattern of a cluster of rods of the precursor Co–La hydroxide, $[Co^{2+}] = [La^{3+}] = 0.002$ *M*. Diffraction rings at 5.51, 3.18, 2.49, 2.23, 1.90, 1.81, and 1.63 Å suggest isomorphism with $La(OH)_3$.

trates (metal concentrations between 2×10^{-3} and 1 *M*) afforded visually homogeneous, olive-green gels. Although powder X-ray diffraction traces of the gels were featureless, suggesting precursor preparations to be poorly crystalline, selected area electron diffraction (SAD) patterns (Fig. 1) indicate a structure which can be indexed on a hexagonal unit cell [$a = 6.51(3)$, $c = 3.81(1)$ Å], isomorphous with that of $La(OH)_3$ [JCPDS No. 36-1481: $a = 6.5286(5)$, $c = 3.8588(5)$ Å]. Omitting the acetone treatment had little effect on degree of crystallinity of the gel, but did alter its decomposition behavior dramatically (see below).

When the co-precipitation was performed in the absence of NaOCl oxidant, a lilac-pink gel resulted. The XRD of a sample washed with deoxygenated water showed intense peaks due to the presence of β-$Co(OH)_2$ [cf. JCPDS file No. 30-443]. On the other hand, dehydration of the gel with acetone resulted in a grey solid, containing only a trace of $Co(OH)_2$. This material was sensitive to subsequent oxidation, so that on standing in air an olive solid was slowly produced.

In the oxidized/co-precipitated gels, transmission electron microscopy indicated two principal morphologies (Fig. 2), each of which afforded a SAD pattern essentially identical to that in Fig. 1. The samples prepared from more concentrated solutions (i.e., $[Co^{2+}] = [La^{3+}] = 0.2$ or 1 *M*) consisted mainly of rod-like particles of approximately constant size (ca. 1×5 nm). Those prepared at lower concentrations (i.e., 0.02 or 0.002 *M*) contained small flakes interspersed with larger rod-shaped particles (up to 1 μm long). Such polymorphism has been reported for both the rare earth and actinide trihydroxides, with rod-like particles appearing at the expense of the flakes as the hydroxide gel is aged (*12–14*). In the present work, the rod-shaped Co–La hydroxide particles grew considerably if left overnight in the mother liquor. In some preparations, large hexagonal outlines were also observed in the micrographs. These were also ascribed to a mixed hydroxide, isomorphous (by SAD) with the crystalline hexagonal form of $La(OH)_3$. It has been reported that such hexagonal-shaped particles can also be formed on aging rod-like Eu- or $Nd(OH)_3$ (*13, 14*).

It is known that CO_2 is readily sorbed by rare earth hydroxide gels (*15, 16*). Similarly, the mixed hydroxide precursors were found to react with atmospheric CO_2, introduced during sample preparation and handling, to exhibit infrared spectral bands at 1475(s), 1384(s), 1053(w), and 850(m) cm^{-1}, assignable to unidentate carbonate ligands, in addition to bands associated with the hydroxyls at 3420 (br) cm^{-1}. Only careful atmospheric control during precipitation and handling minimized carbonate contamination.

Perovskite Formation

Thermal behavior of the precursors was examined by TGA and DTA (Fig. 3). In the case of the material prepared in the presence

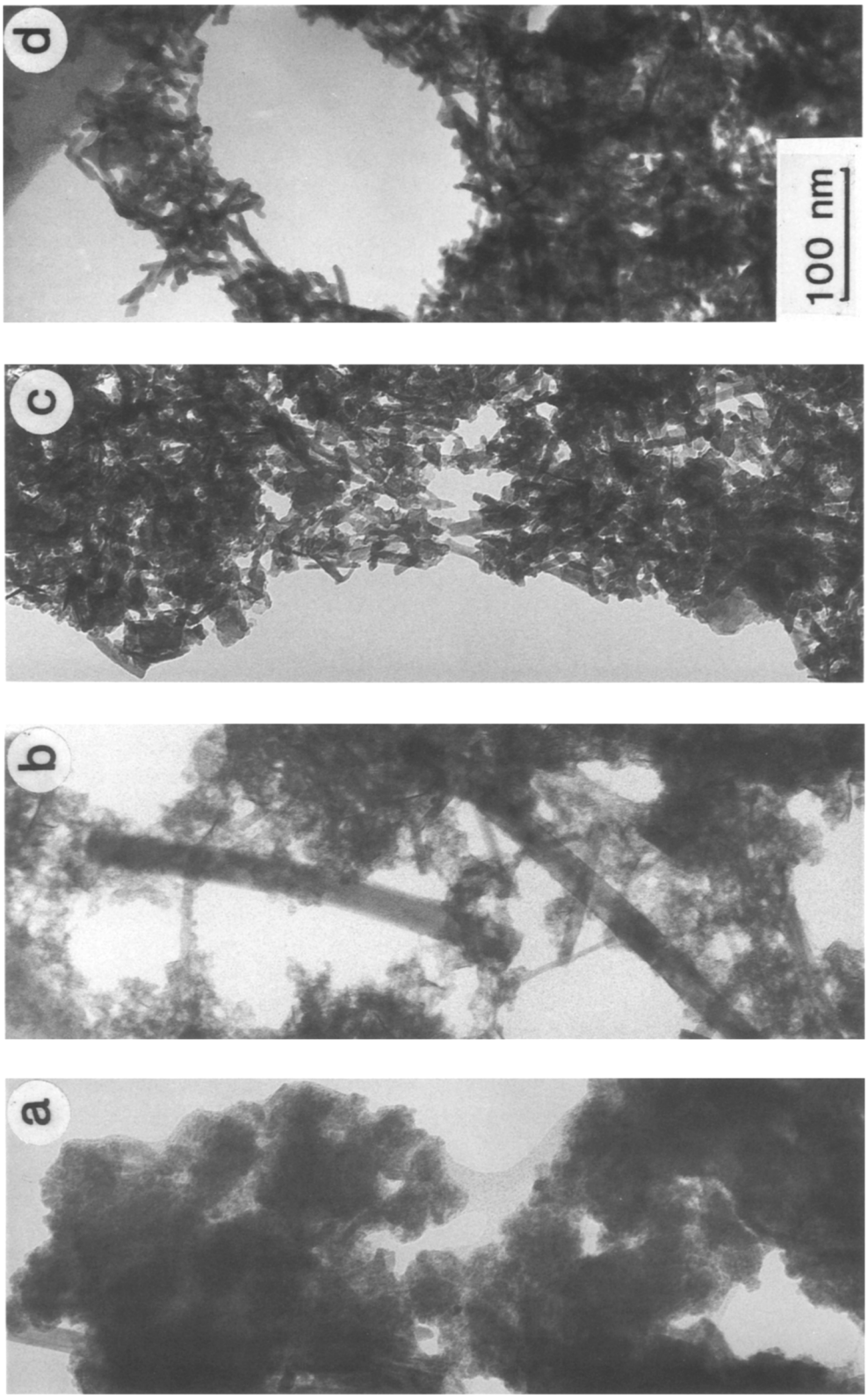
d
100 nm
c
b
a

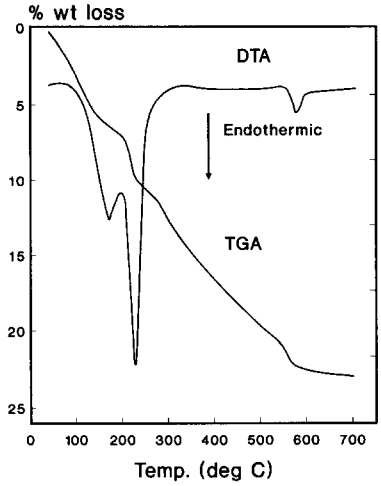

FIG. 3. TGA and DTA of Co–La hydroxide, $[Co^{2+}] = [La^{3+}] = 0.02\ M$.

of NaOCl and treated with acetone, a strong endothermic double peak around 150–250°C in the DTA corresponded to weight losses in the TGA primarily due to dehydration. A mass spectrum of the evolved gases revealed only traces of acetone released during the early stages of heating. Similar results were obtained for the TGA on samples prepared in the absence of added NaOCl (but which had oxidized on standing in air).

Crystallization to the perovskite was associated with a small endotherm in the DTA just below 600°C. The accompanying small but abrupt weight loss arises from CO_2 liberation (*16*). Sometimes, when substantial carbonate contamination was present, weight losses were also observed by TGA up to 750°C. Formation of crystalline $LaCoO_3$ at 600°C was confirmed by XRD (Fig. 4) and at 650°C by TEM and electron diffraction (Fig. 5). Sharp, well-defined perovskite XRD peaks were observed when precursors, co-precipitated at low La and Co concentrations (0.002 and 0.02 *M*) were calcined. From precursors, co-precipitated at higher concentrations (0.2 and 1 *M*) substantially broader XRD peaks resulted, indicating smaller crystallite sizes. From precursors co-precipitated at the higher concentrations of 0.2 *M* and, in particular, 1 *M*, traces of Co_3O_4 were evident in the XRD of samples heated to 650°C and traces of La_2O_3 at 750°C. Omission of the acetone treatment step had a deleterious effect on the crystallite dimensions (Fig. 6a), producing a wide range of sizes (up to 1 μm after heating to 600°C). In contrast, acetone washing afforded a much more uniform size distribution of particles (Fig. 6b), considerably smaller in size (20 nm) after heating to 600°C (1 h). The difference in particle size is reflected in the surface areas of the samples.

Surface Areas

The maximum surface area obtained was 43 m^2/g for a crystalline sample heated in air for 1 h at 400°C and for a further hour at 600°C. IR spectroscopy indicated slight carbonate contamination on this sample, which was removed by further heating at 650°C for 1 h. However, this treatment reduced the surface area to 30 m^2/g. Nitrogen adsorption–desorption measurements on a sample heated to 650°C gave a fully reversible, Type II isotherm. The absence of any hysteresis indicates the perovskite powder was free of mesopores (*17*).

Major effects of varying preparative conditions are seen in the resultant surface areas of the perovskite after heating to 600°C (1 h). Thus, omission of NaOCl oxidant afforded a material with an area of only 19 m^2/g, whereas a sample dehydrated by air-drying, rather than washed with acetone, gave an area of only 9 m^2/g. Precursors co-precipitated at high La and Co concentrations resulted in perovskite samples with higher surface areas,

FIG. 2. Transmission electron micrographs of Co–La hydroxide prepared at different starting metal concentrations. (a) $[Co^{2+}] = [La^{3+}] = 0.002\ M$, (b) 0.02 *M*, (c) 0.2 *M*, and (d) 1 *M*.

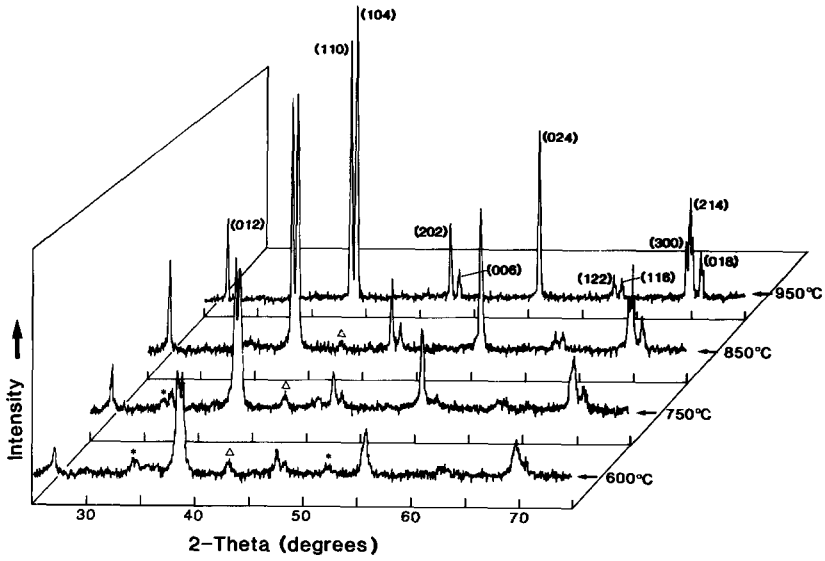

FIG. 4. XRD powder patterns of $LaCoO_3$, $[Co^{2+}] = [La^{3+}] = 0.2\ M$, heated to various temperatures, showing the evolution of crystallinity with increasing temperature. Impurity peaks: (△) Co_3O_4, (*) La_2O_3.

at the same calcination temperature, than those co-precipitated at low La and Co concentrations (Table 2).

The BET surface area of $LaCoO_3$ was dependent upon the maximum calcination temperature between 600 and 950°C. The area decrease, indicating the ease with which the unsupported $LaCoO_3$ powders sintered, was paralleled by an increase in sample crystallinity as determined by X-ray diffraction (Fig. 4). Crystallite size, calculated from the Debye–Scherrer equation, enabled an independent estimate of the surface area. These areas (Fig. 7) correlate well with that determined from gas adsorption for moderate values, but discrepancies at low areas are an indication that the oxide particles are polycrystalline.

Catalytic Activity

The comparative activities of $LaCoO_3$ samples, pretreated at 600, 650, 750, and 850°C, were measured for the following reactions:

$$CO + \tfrac{1}{2}O_2 \rightarrow CO_2 \qquad (1)$$

$$C_3H_8 + 5O_2 \rightarrow 3CO_2 + 4H_2O. \qquad (2)$$

The experiments were carried out in a temperature-programmed mode, between RT and 600°C, using a dilute CO/propane/O_2 gas mixture, with a composition typical of that encountered in automotive exhaust gas streams.

As illustrated in Fig. 8, CO_2 formation occurred in two distinct steps with the step at lower reaction temperatures arising from CO oxidation and that at higher temperature from propane total oxidation. The results in Table 3 show that as the surface areas of the powders increased, catalytic activity also increased, requiring lower reaction temperatures to completely oxidize CO and propane.

The areal activities of $LaCoO_3$ for the two reactions were determined. The amount of CO and propane oxidized at two set temperatures followed a linear relationship with surface area (Fig. 9). These activities were found to be $0.08 \pm 0.04\ cm^3\ m^{-2}\ min^{-1}$ for CO oxidation at 180°C and $0.01 \pm 0.003\ cm^3\ m^{-2}\ min^{-1}$ for propane oxidation at 340°C, under the conditions and gas compositions

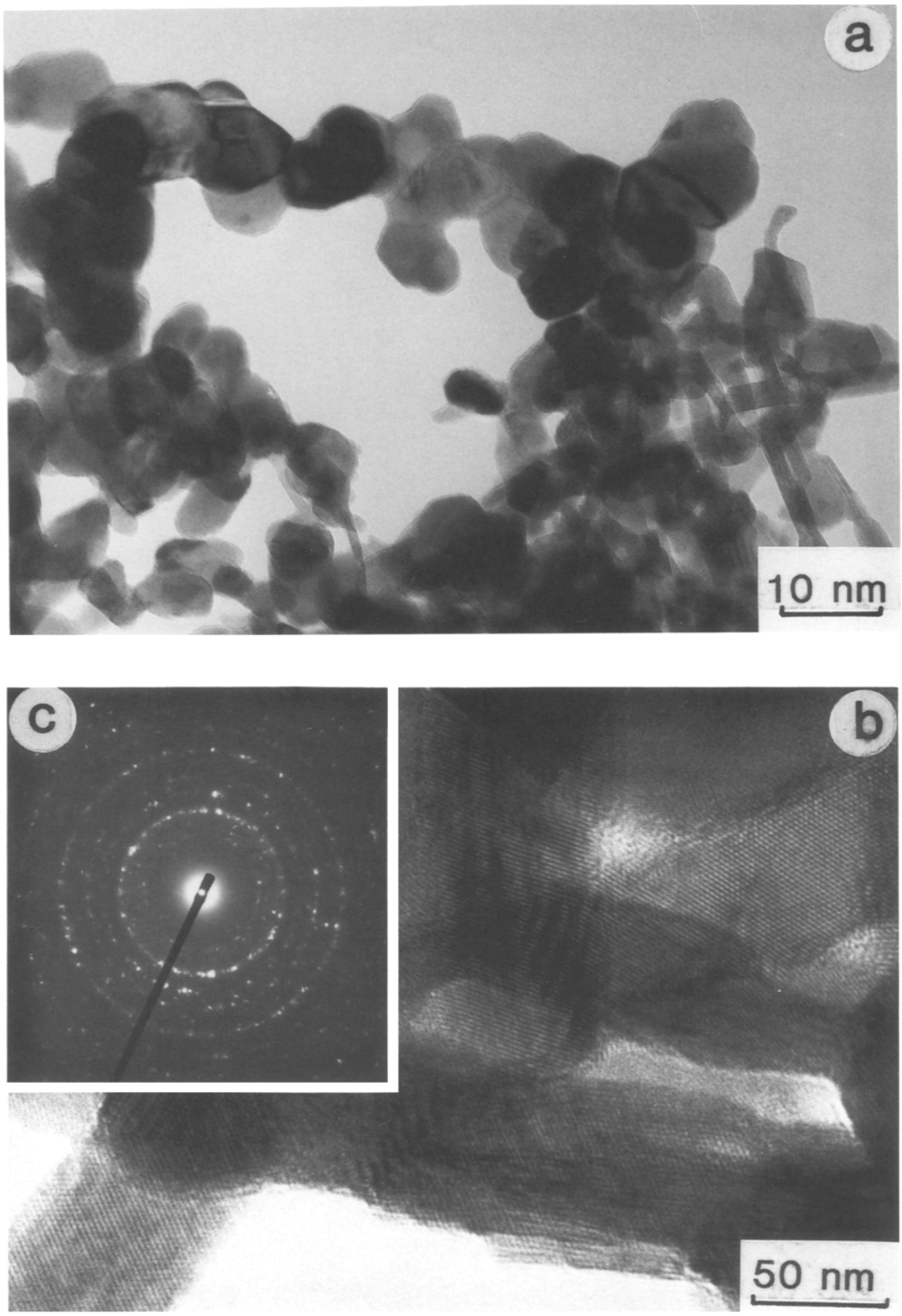

FIG. 5. Transmission electron micrographs of $LaCoO_3$ calcined at 650°C, $[Co^{2+}] = [La^{3+}] = 0.2\ M$. Sintering of the particles by "necking" is evident in (a). Lattice images in (b) and the SAD pattern (c), with prominent spots at 3.78, 2.65, 2.17, 1.90, 1.54, and 1.18 Å, confirm the formation of $LaCoO_3$ phase [cf. JCPDS No. 25-1060].

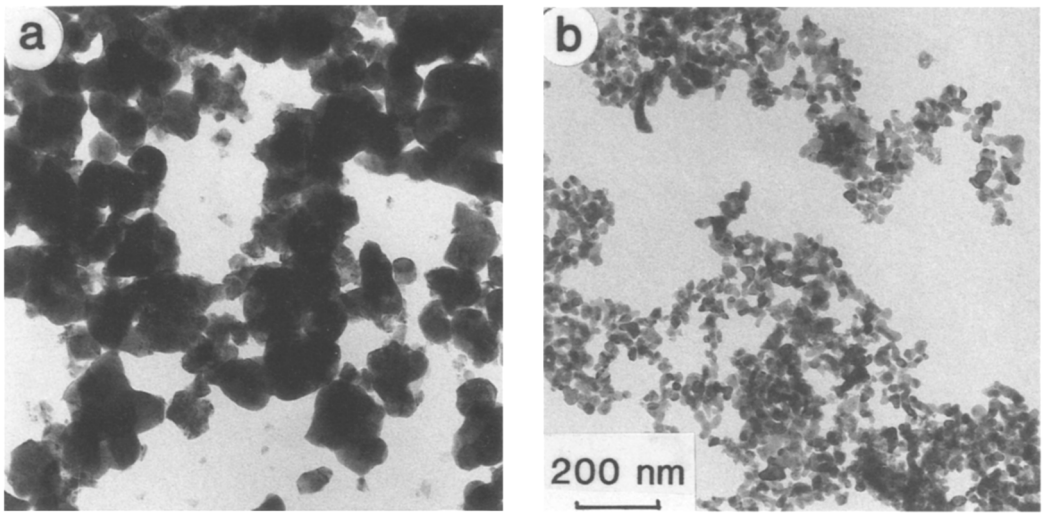

FIG. 6. Transmission electron micrographs of $LaCoO_3$ calcined at 600°C, $[Co^{2+}] = [La^{3+}] = 0.02\ M$, showing the effect on particle size of washing the precusor gel with (a) water only and (b) water, then acetone.

used in this study. These values correspond to turnover numbers for CO and propane of 5×10^{-3} and 6×10^{-4} molecules oxidized per atom of surface Co per second, respectively (for $LaCoO_3$, the number of Co atoms was estimated to be 6.8×10^{18} m^{-2} on an exposed {100} plane).

Low levels of sodium (<0.1%) present in the calcined perovskite did not appear to promote the oxidation reaction. Thus, sam-

TABLE 2

Effect of La and Co Co-precipitation Concentrations on Perovskite Surface Area

Conc. (*M*)	Treatment temp. (°C)[a]	BET surface area (m^2/g)	Phases[b]
0.002	600	12	*P*
	670	8	*P*
	750	6	*P*
0.02	670	14	*P*
	750	7	*P*
0.2	600	32	*P*, La_2O_3(tr), Co_3O_4(tr)
	650	22	*P*, La_2O_3(tr), Co_3O_4(tr)
	750	13	*P*, La_2O_3(tr), Co_3O_4(tr)
	850	6	*P*, Co_3O_4(tr)
1.0	750	14	*P*, La_2O_3, Co_3O_4

[a] Calcined at specified temperature for 1 h.
[b] Crystalline phases observed by XRD; *P*, $LaCoO_3$; tr, trace.

ples of $LaCoO_3$, prepared by a sodium-free route, using Me_4NOH/H_2O_2 instead of NaOH/NaOCl and calcined at 650 or 850°C, exhibited almost the same catalytic activity per unit surface area as that of samples prepared in the presence of sodium ions.

DISCUSSION AND CONCLUSIONS

The method of co-precipitation/oxidation employed in this work for the preparation of $LaCoO_3$ was similar to that used by Vidyasagar *et al.* for the synthesis a range of complex metal oxides (*18*). The major difference lies in the means of subsequent dehydration of the gel; rather than simply heating the washed gel in air, it was first partially dehydrated by use of acetone. Such controlled dehydration of hydrogels, using water-miscible solvents, has been shown to produce high-area SiO_2 (*19*), Al_2O_3 (*20*), and ZrO_2/TiO_2 (*21*) from their respective hydrogels. Displacement of water by acetone in such a gel leads to a lowering of surface tension and smaller capillary forces, producing weaker agglomeration and maintenance of a more open structure of hydroxide particles on drying. The result is less pore collapse on calcination (*20*).

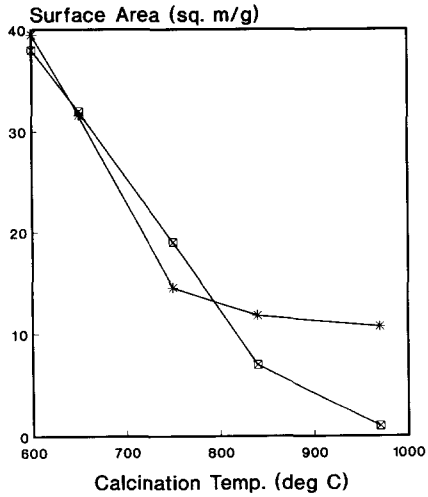

FIG. 7. Effect of calcination temperature on the surface area of $LaCoO_3$, $[Co^{2+}] = [La^{3+}] = 0.2\ M$. From BET (⊠); from XRD (*).

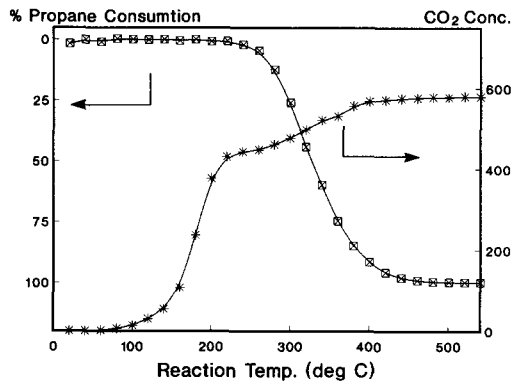

FIG. 8. Catalytic activity of $LaCoO_3$, from $[Co^{2+}] = [La^{3+}] = 0.2\ M$, towards oxidation of mixtures of CO and propane with increasing reaction temperature. CO_2 concentration in gas stream (⊠) (μmol/liter), percentage of total propane consumed (*) as a function of reactor temperature. Temperature ramp rate = 4°C/min, initial [CO] = 439 μmol/liter, initial $[C_3H_8] = 46.4$ μmol/liter. The inflection in the CO_2 curve corresponds to the temperature at which consumption of CO is complete.

The initial, mixed Co/La hydroxide coprecipitate consists of a poorly crystalline mixed hydroxide of Co(II), Co(III), and La, isomorphous with $La(OH)_3$. This assumption is based on the following observations:

(i) Selected area electron diffraction patterns of the precursor suggest that the mixed Co/La hydroxide crystallizes with a disordered $La(OH)_3$ structure.

(ii) The relatively low temperature of conversion to the perovskite indicates a precursor material with Co and La in intimate contact.

(iii) It appears that oxidation of the Co(II) to Co(III) was incomplete during initial precipitation, as the products had an olive-green coloration characteristic of Co(II) (cf. green color of CoO), rather than the brown or black of "$Co_2O_3 \cdot aq$" or CoO(OH) (*22*). On exposure of a vacuum-dried powder to air, oxidation of Co(II) proceeded further to afford the characteristic brown color of a Co(III) oxide.

(iv) The mode of thermal decomposition of the mixed Co/La hydroxide is similar to $La(OH)_3$, prepared by an analogous precipi-

TABLE 3

Effects of Perovskite Surface Area on Catalytic Activity[a]

% Conversion	Surface area (m^2/g)			
	32	22	13	6
	Reaction temperature (°C)			
A. Extent of CO oxidation				
0	40	40	40	40
2	77	84	109	148
25	142	161	170	195
50	160	179	185	210
75	171	192	197	223
98	201	221	232	256
100	212	232	246	265
B. Extent of propane oxidation				
00	195	220	220	270
02	225	239	252	287
25	278	299	310	349
50	305	320	347	385
75	334	362	385	425
98	418	440	478	518
100	520	540	560	600

[a] Starting Co and La concentrations were 0.2 *M*.

tation/dehydration route (*24*), undergoing a distinct two-step endothermic dehydration between 100 and 300°C. The final small and abrupt endothermic loss, below 600°C, corresponding to CO_2 from a carbonate impurity, is analogous to the behavior of $La(OH)_3$ (*23, 24*).

(v) The IR spectrum of the vacuum-dried mixed precursor exhibited a broad peak centered around 3400 cm^{-1} rather than the two distinct bands around 3600 cm^{-1} as found in $La(OH)_3$ (*23, 24*). It is likely that there is a greater range of structural environments for the hydroxyls in the mixed precursor, as would be expected of a poorly crystalline material.

The hydroxide gels prepared here are considerably less crystalline, as indicated by XRD, than the mixed Co/La hydroxide phase, previously reported by Vidyasagar and co-workers (*18*). This difference is probably due to variations in the washing and aging steps. Figure 6 shows that the perovskite particles formed by calcination of the precursor were substantially smaller after gel treatment with acetone than without it. A better understanding of the effects of such experimental parameters is complicated by the range of particle morphologies possible in the precursor gels. It remains to be established whether the morphological differences significantly affect either decomposition behavior or catalytic performance.

Carbonate bands observed in the infrared spectrum indicate that carbon dioxide adsorption results in the formation of hydroxy carbonate species, akin to $La_2(OH)_{6-2x}(CO_3)_x$ (*25*). This material decomposes to a Co-doped analogue of $La_2O_2CO_3$ upon heating. The detrimental effect of such carbonate formation on the surface area of the perovskite results from the higher calcination temperatures required for its removal. The extra precautions involved in controlled atmosphere synthesis should be considered worthwhile when preparing rare earth oxide-containing derivatives. With sufficient care, the final product can be obtained comparatively free of carbonate contamination. Under such conditions it is possible to produce perovskites with relatively high surface areas. The resultant perovskite exhibits

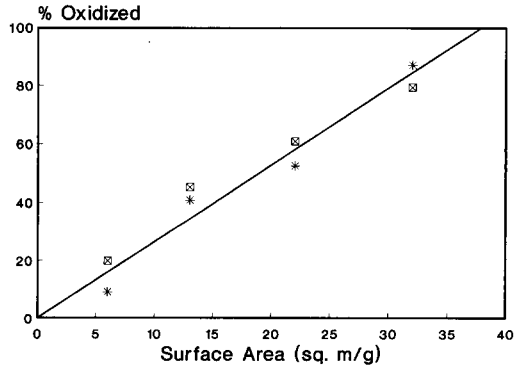

FIG. 9. Dependence of percentage CO and propane oxidation on the total BET surface area of $LaCoO_3$, $[Co^{2+}] = [La^{3+}] = 0.2$ *M*. (⊠) percentage CO converted at 180°C; (*) percentage propane converted at 340°C.

no micro- or mesoporosity, with the external surface area of the crystallites defining the overall area available.

The activities obtained for the oxidation of CO and propane (Table 3) over $LaCoO_3$, in the temperature range RT to 600°C, varied linearly with surface area (Fig. 9). For a high-area perovskite (32 m^2/g), 160°C was the temperature at which the CO conversion reached 50% ($T_{50\%}$). This temperature was 50°C higher for the sample with an area of only 6 m^2/g. The corresponding difference for propane was 80°C. Activities were comparable to those found by other workers, when differences in experimental protocol are borne in mind (*26, 27*). Thus, from the data of Nakamura *et al.*, obtained in a flow system under isothermal conditions (150 and 227°C, with a vol% gas composition of CO (or propane) : O_2 : N_2 = 0.83 : 33.3 : balance), 12.6% of the CO is oxidized at 150°C and 1.5% of the propane is totally oxidized at 227°C (*26*). The corresponding values for our catalyst (calcined at 650°C), run under temperature-programmed rather than isothermal conditions at these set temperatures, are 32.5% for CO and 2.3% for propane.

Efforts are now directed to preparing more active Sr-doped phases and to increasing the surface area of perovskite powders produced by this co-precipitation/oxidation method by decreasing the precursor particle size even further.

ACKNOWLEDGMENTS

We thank Dr. D. Hay for X-ray diffraction and Dr. P. de Munk for surface area measurements, Messrs. D. Watson and H. Jaeger for the electron microscopy and diffraction, and Dr. L. A. Bruce for helpful discussions.

REFERENCES

1. Tseung, A. C. C., and Bevan, H. Y., U.S. Patent 3,922,204.
2. R. J. H. Voorhoeve, *in* "Advanced Materials in Catalysis" (J. J. Burton and R. L. Garten, Eds.), p. 129. Academic Press, New York, 1977.
3. Yao, Y. F., *J. Catal.* **36,** 266 (1975).
4. Gallagher, P. K., Johnson, D. W., Remeika, J. P., Schrey, F., Trimble, L. E., Vogel, and E. M., Voorhoeve, R. J. H., *Mater. Res. Bull.* **10,** 529 (1975).
5. Nakamura, T., Misono, M., and Yoneda, Y., *Chem. Lett.*, 1589 (1981).
6. Wachowski, L., *Surf. Coat. Technol.* **29,** 303 (1986).
7. Tanaka, K., Nishida, T., and Imamura, S., *Chem. Express* **2,** 759 (1987).
8. Tascón, J. M. D., Mendioroz, S., and González Tejuca, L., *Z. Phys. Chem.* **124,** 109 (1981).
9. Zhang, H., Teraoka, Y., and Yamazoe, N., *Chem. Lett.*, 665 (1987).
10. Imai, H., Takami, K., and Naito, M., *Mater. Res. Bull.* **19,** 1293 (1984).
11. Tseung, A. C. C., and Bevan, H. L., *Electroanal. Chem. Interfac. Electrochem.* **45,** 429 (1973).
12. Haire, R. G., Lloyd, M. H., Milligan, W. O., and Beasley, M. L., *J. Inorg. Nucl. Chem.* **39,** 843 (1977).
13. Milligan, W. O., and Dwight, D. W., *J. Electron Micros.* **14,** 264 (1965).
14. McBride, J., Laboratory studies of sol-gel process at the Oak Ridge National Laboratory, ORNL-TM-1980, 1967.
15. Rosynek, M. P., and Magnuson, D. T., *J. Catal.* **48,** 417 (1977).
16. Alvero, R., Odriozola, J. A., Trillo, J. M., and Bernal, S., *J. Chem. Soc. Dalton Trans.*, 87 (1984).
17. Gregg, S. J., and Sing, K. S. W., "Adsorption, Surface Area and Porosity," 2nd Ed., p. 41. Academic Press, London, 1982.
18. Vidyasagar, K., Gopalakrishnan, J., and Rao, C. N. R., *J. Solid State Chem.* **58,** 29 (1985).
19. Iler, R., "The Chemistry of Silica." Wiley, New York, 1979.
20. Dombro, R. A., and Kirsch, W., Eur. Pat. Application, 110,078 (1984).
21. White, A., Walpole, A., Huang, Y., and Trimm, D. L., *Appl. Catal.* **56,** 187 (1989).
22. Nicholls, D., *in* "Comprehensive Inorganic Chemistry" (J. C. Bailar *et al.*, Eds.), Vol. III, p. 1094. Pergamon Press, Oxford, 1973.
23. Rosynek, M. P., and Magnuson, D. T., *J. Catal.* **46,** 402 (1977).
24. Bruce, L. A., Hardin, S., Hoang, M., and Turney, T. W., "Synthesis and Properties of Highly Disperse Rare Earth Oxides," CSIRO C-DMST Report No. 89-24, 1989.
25. Bernal, S., Diaz, J. A., Garcia, R., and Rodriguez-Izquiero, J. M., *J. Mater. Sci.* **20,** 537 (1985).
26. Nakamura, T., Misono, and M., Yoneda, Y., *J. Catal.* **83,** 151 (1983).
27. Mizuno, N., Fujii, H., and Misono, M., *Chem. Lett.*, 1333 (1986).